

# Effect of Spacer on the Fabrication and Properties of TiZr-Based BMG Foams for Bio-Implant Applications

Muhammad Jauharul Maqnun<sup>1\*</sup>, Jason Shian-Ching Jang<sup>1,2</sup>, I Yu Tsao<sup>1</sup>, Han-Lin Tsai<sup>1</sup>, Chao-Yu Shen<sup>1</sup>, Pei-Chun Wong<sup>3</sup> and Jia-Lin Wu<sup>3</sup>

<sup>1</sup>Institute of Materials Science and Engineering, National Central University, Taiwan

<sup>2</sup>Department of Mechanical Engineering, National Central University, Taiwan

<sup>3</sup>Department of Orthopedics, Taipei Medical University, Taiwan

\*Corresponding author: Muhammad Jauharul Maqnun, Institute of Materials Science and Engineering, National Central University, Taiwan



## ARTICLE INFO

**Received:**  March 15, 2022

**Published:**  March 25, 2022

**Citation:** Muhammad Jauharul Maqnun, Jason Shian-Ching Jang, I Yu Tsao, Han-Lin Tsai, Chao-Yu Shen, et al., Effect of Spacer on the Fabrication and Properties of TiZr-Based BMG Foams for Bio-Implant Applications. Biomed J Sci & Tech Res 42(5)-2022. BJSTR. MS.ID.006821.

**Abbreviations:** BMG Foam; Spacer Holder; Hot-Pressing; Biomaterials

## ABSTRACT

Biocompatible TiZr-based BMG foams (with the composition of  $Ti_{42}Zr_{35}Si_5Ta_3Co_{12.5}Sn_{2.5}$  in at. %) were successfully fabricated by using Cu spacer particles. The TiZr-based BMG powder mixed with Cu spacer particles in the various ratio of volume fractions based on the desired porosity. The mixed powder was then processed by a hot pressing machine in 300 MPa of pressure, 520°C temperature, and 5 minutes of holding time. The porous sample was obtained after removing Cu spacer particles with a 50:50 concentrated  $HNO_3:H_2O$  mixed solution at room temperature. By SEM examination, the porosity parameters of fabricated porous samples were confirmed similar to the human bones (100-325  $\mu m$ ) which resulting in pore sizes of 120  $\mu m$ . The XRD and TEM analysis exhibit that the porous samples retain their amorphous state after the hot pressing process. Similar mechanical properties to the human bones can be obtained by controlling the porosity of the samples based on the Gibson and Ashby model. Increasing porosity of the samples from 2% to 67.9% confirmed a decrease in the compressive strength (from 1261 to 76 MPa) and Young's modulus (from 79.7 to 4.6 GPa). In the biocompatibility test, the fabricated porous sample by using Cu spacer particles shows that cell viability increased with increasing incubation time which means that the cell was growing continuously. After 8 h incubation, the cell migration was observed and showing a distance reduction of approximately 600  $\mu m$ . The results of calcium deposition rate are always higher than 100% show that the sample positively biocompatible in the human body.

## Introduction

Titanium-based alloys have become a basic choice of metallic materials for orthopedic implants because of their attractive properties, such as excellent mechanical properties, high corrosion resistance, and good biocompatibility [1-3]. However, there are complications in many cases after implantation of orthopedics for example aseptic loosening and prosthetic joint infection. Also, it was reported that Al and V ions released from Ti-6Al-4V alloy thus causing long-term health problems like Alzheimer's disease,

neuropathy, and osteomalacia [4]. Further, another main issue that makes Ti-based alloys unsuitable for bio-implant materials is a mismatch in Young's modulus between implants and natural bone. The Young's modulus of this alloy over 100 GPa, which is this value higher than human bone's (1-35 GPa) [5]. This mismatch could cause stress shielding, resulting in bone resorption and loosening of the implant after a period of implantation [6].

Recent studies have found that lower Young's modulus can be obtained by the development of titanium-based BMG since

amorphous alloy shows special properties than conventional crystalline materials such as higher mechanical strength, corrosion resistance, and wear resistance [7-8]. Even though Ti-based BMG indicates good mechanical properties with high strength (1800-2500 MPa) and low Young's modulus (90-110 GPa), but the glass-forming ability (GFA) of most Ti-based BMG alloys still need to improve [9-11]. Some studies show that adding the Zr element in TiZr-based BMG alloy can make GFA increased without reducing other properties [12-14]. Our previous studies [15-16] reported biocompatible TiZr-based BMGs with the composition of  $Ti_{42}Zr_{35}Si_5Ta_3Co_{12.5}Sn_{2.5}$  were fabricated by the hot-pressing method. The spacer holder method was selected for fabricating bulk samples and then removed to generate porous samples. Both mechanical properties and biocompatibility results show this material has similar properties to human bones. The purpose of this study is to continue the above studies were before use NaCl and Al particles as spacer holders. The Cu particle is chosen for the new spacer particle because of its higher thermal conductivity than NaCl and Al particles. Then, we can conclude that using higher thermal conductivity as a spacer particle during hot pressing can strengthen the bonding interface between BMG particles.

## Materials and Methods

### Sample Fabrication

The TiZr-based MG powders with a chemical composition of  $Ti_{42}Zr_{35}Si_5Ta_3Co_{12.5}Sn_{2.5}$  and particle sizes of less than 25  $\mu m$  are selected to fabricate porous samples. Then, the spacer holders (Cu particles) with a larger size (100-120  $\mu m$ ) are mixed in with a determined ratio of volume fractions. Based on the previous studies, the optimal parameter to fabricate TiZr-based BMG foam samples using a hot pressing machine are 300 MPa of hot pressing pressure, 520°C of hot pressing temperature, and 5 minutes of holding time [15-16]. Finally, the prepared sample needs to remove the spacer holder to produce a porous sample using a 50:50 concentrated  $HNO_3:H_2O$  mixed solution at room temperature for 3 days.

### Morphology

The SEM equipment (Inspect F50, Thermo Fisher Scientific Inc.) which operated at 20 keV was used to observe the pore sizes and morphology of TiZr-based BMG foams. Each porous sample of TiZr-based BMG foams is then taken SEM images with 500 $\times$  magnification during the SEM experiment. From the result of SEM images, the pore size and morphology of each sample known by observing the diameter of the connecting cavity.

### Microstructure Characterization

The XRD (D2 PHASER X-ray diffractometer; operated at 40 kV) and transmission electron microscopy (TEM; JEOL JEM2100;

operated at 200 keV) were used to characterize an amorphous structure of the TiZr-based BMG foams. A focused ion beam system (FEI Versa 3D Dual Beam; operated at 30 kV) is used to prepare a thin foil specimen from the aforementioned porous sample. Thin foil sample then carry out by FIB milling at 4 keV and angle incident of 5°.

### Mechanical Properties

The MTS machine (HUNG TA Instrument HT-9102) was used to determine the mechanical properties of the TiZr-based BMG foams, including compressive strength and Young's modulus. The porous samples for the compression test were cut in a rectangular shape with a size of 2.5  $\times$  2.5  $\times$  5 mm ( $\pm$ 0.1 mm) by using a low-speed diamond saw machine (ISOMECH, BUEHLER). Then, the sample was put into the steel mold to perform a compression test with a constant strain rate of  $1 \times 10^{-4}$  mm/s at room temperature.

### Biocompatibility Test

MC3T3-E1 pre-osteoblasts were used to performed cell viability by 3-(4,5-dimethylthiazol-2-yl)-2,5-diphenyl tetrazolium bromide (MTT) assay with the indirect method. MC3T3-E1 pre-osteoblasts were first cultured in  $\alpha$ -MEM with 10% fetal bovine serum (Gibco®). 100  $\mu l$  of MC3T3-E1 pre-osteoblast suspension was added into a 96-well culture plate with the cell density of 5000 cells/well and preincubated for 24 h at 37°C in a 5%  $CO_2$  atmosphere. After cell attachment, replaced culture medium by 100  $\mu l$  of one of three precipitate media for incubation in the same environment for 1, 3, and 7 days. Subsequently, 10  $\mu l$  of MTT solution (Invitrogen, US) was added to each well and incubated for 3 h. After that, removed all of the solutions and added 100  $\mu l$  of dimethylsulfoxide (DMSO) to dissolve formazan crystals, and the optical density (OD) was detected by a microplate reader with the wavelength of 560 nm (Multiskan FC; Thermo, Waltham, MA, USA).

The migration capacity of MC3T3-E1 pre-osteoblasts was executed by scratch assay with the simulation of the precipitate medium. MC3T3-E1 pre-osteoblasts suspension (5000 cells) was added into a 24-well culture plate for 24 h incubation. A straight line was scratched by the tip of a 1000- $\mu l$  pipet along the monolayer of cells. Removed the cell debris with culture medium gently. 500  $\mu l$  of the precipitate medium was added to each well for incubation. After 8 h of incubation, observed and captured the cells images by optical microscope (Primovert; Zeiss, Germany). Extracellular calcium deposition of MC3T3-E1 pre-osteoblasts was analyzed by alizarin red S (ARS) staining. First, 500  $\mu l$  of MC3T3-E1 pre-osteoblasts suspension was seeded into a 24-well culture plate with a cell density of 5000 cells/well. After 24 h incubation, replaced the culture medium with the precipitate medium for 21 days of incubation. Before staining, removed the precipitate medium and

gently rinsed with PBS three times. After that, fixed the cell with 4% of paraformaldehyde for 15 minutes at room temperature. Removed the fixative and stained the ECM calcium with ARS dye for 20 minutes at room temperature. The ARS dye has been removed and captured by the images of an optical microscope (Primovert; Zeiss, Germany).

## Results and Discussion

### Removal of Spacer Particles

The Cu particle from the prepared samples was removed with a 50:50 concentrated  $\text{HNO}_3:\text{H}_2\text{O}$  mixed solution at room temperature for 3 days. However, the bigger size of the samples needs more time to completely remove the Cu particle. So, some of the experiments require the porous samples removed up to 7 days, such as SEM,

TEM, and biocompatibility test. The porous samples were cleaned in immersed ethanol by using an ultrasonic cleaner to avoid contamination with the chemical reaction after the spacer particles removal process (Figure 1).

### Morphology

The morphology of the TiZr-based BMG foams was observed with SEM. The morphologies with real porosity of 11.1%, 27.6%, 40.4%, and 51.0% which fabricated by using Cu spacer particles are shown in Figure 1. SEM images show that the pore size and morphology of the TiZr-based BMG foams were similar to the size of Cu spacer particles (100-120  $\mu\text{m}$ ). Furthermore, the resulted pore size of porous samples in this study in line with the optimal implant-bone for scaffolds *in vitro* which range pore size from 100-325  $\mu\text{m}$  [17] (Figures 2 & 3).

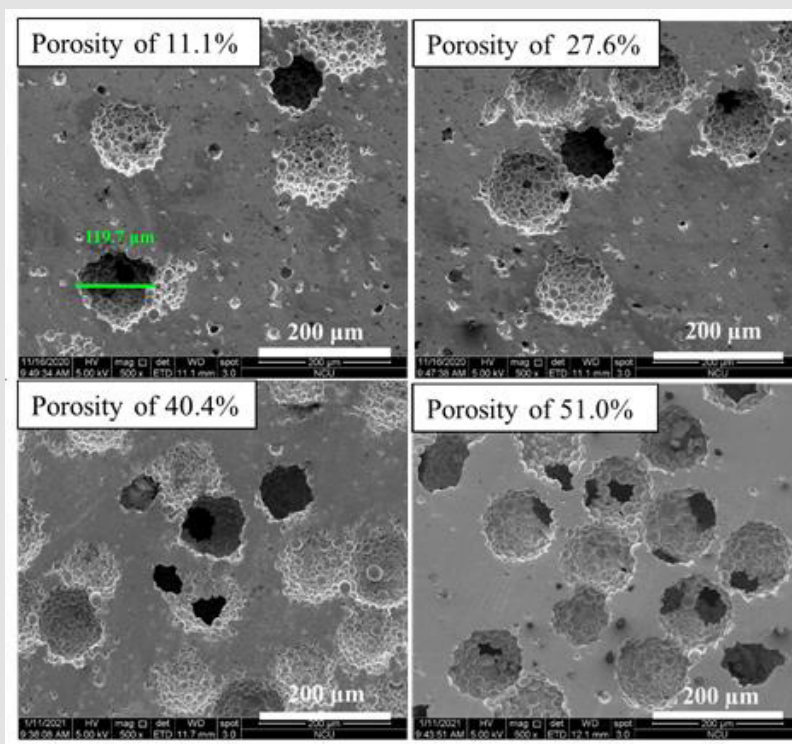


Figure 1: SEM images of TiZr-based BMG foams with different real porosities.

### Microstructure Characterization

The XRD patterns of TiZr-based BMG foams fabricated by using Cu spacer particles were presented in Figure 2. The porous samples were prepared for XRD after hot pressing and spacer particles removal process. All of the samples with different porosities resulting natural amorphous structure with normal broad humps over the  $2\theta$  of around  $30^\circ$ - $50^\circ$ . This shows that the selected hot pressing parameters were successfully to avoid crystalline transformation after the hot pressing process. Figure 3 shows the

bonding interfaces between amorphous alloy particles by TEM images of TiZr-based BMG foams with real porosity of 11.1%. Figure 3a resulted in selected area electron diffraction (SAED) patterns which show typical hollow rings. This proves that the amorphous structures from the fabricated sample retained their amorphous structures during hot pressing. Moreover, the TiZr-based BMG foams forming a strong bonding-force interface between the amorphous alloy particles after the hot pressing process. However, a few lattices appeared in the almost fully amorphous phase. This means that the observed sample cannot avoid the occurrence of

nanocrystallization based on the selected hot pressing parameter. The nanocrystallization zones were observed along with the interfaces between the amorphous alloy particles in the nearly amorphous phase. These nanocrystalline phases contained the

normal  $\alpha$ -Ti phase (hcp structure) and  $\beta$ -Ti phase (bcc structure) with a lattice constant of 0.253 and 0.319 nm, respectively, as shown in Figure 3b, (Figure 4 and Table 1).

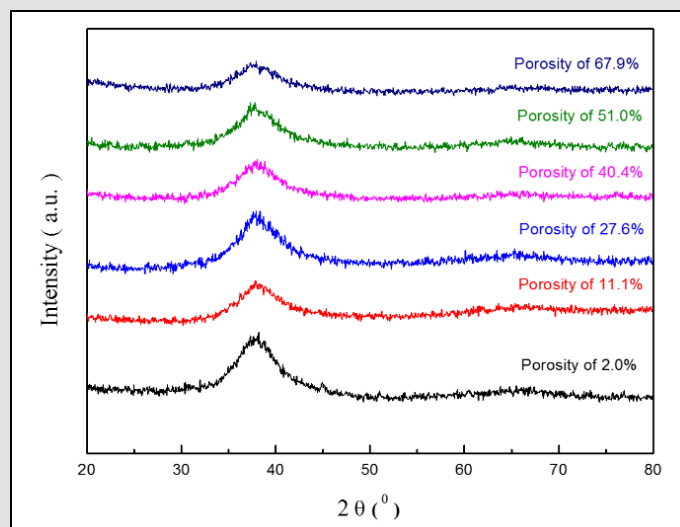


Figure 2: XRD patterns of TiZr-based BMG foams with different real porosities.

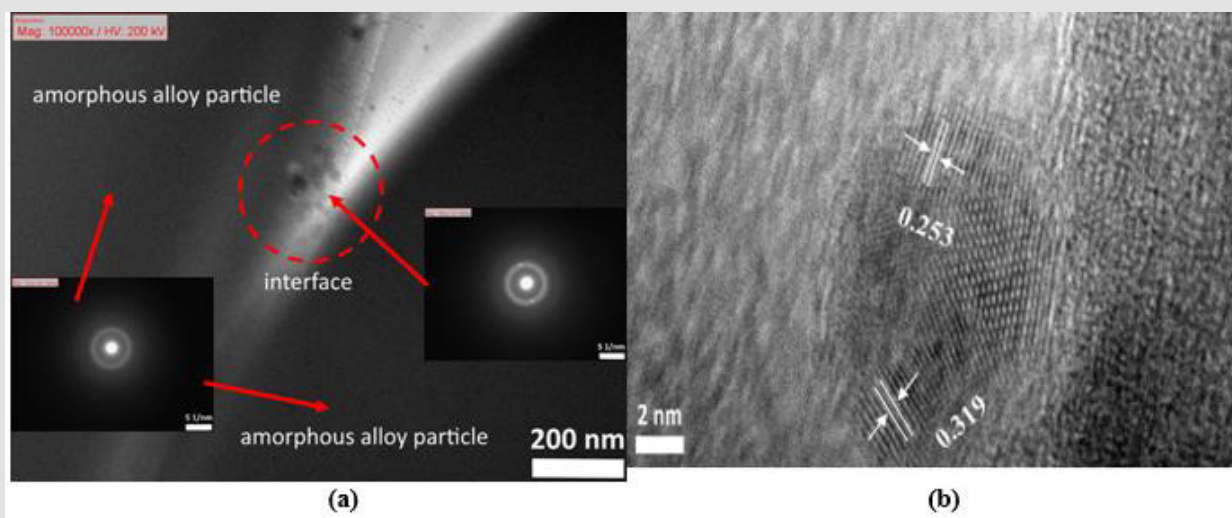


Figure 3: TEM images of TiZr-based BMG foam in real porosity of 11.1% which showing (a) SAED patterns and (b) Nanocrystallization zone.

## Mechanical Properties

Figure 4 presents the compression stress-strain curves of the TiZr-based BMG foams in various porosities. Whereas, the mechanical properties showed in Table 1. These results indicate that increasing porosity of the samples can decrease compressive

strength and Young's modulus. The increasing porosities from 2% to 67.9% resulting in decreased compressive strength and Young's modulus from 1261 to 76 MPa and from 79.7 to 4.6 GPa, respectively. The aforementioned results indicate that the desired mechanical properties can be obtained by controlling the porosity of the samples (Figure 5).



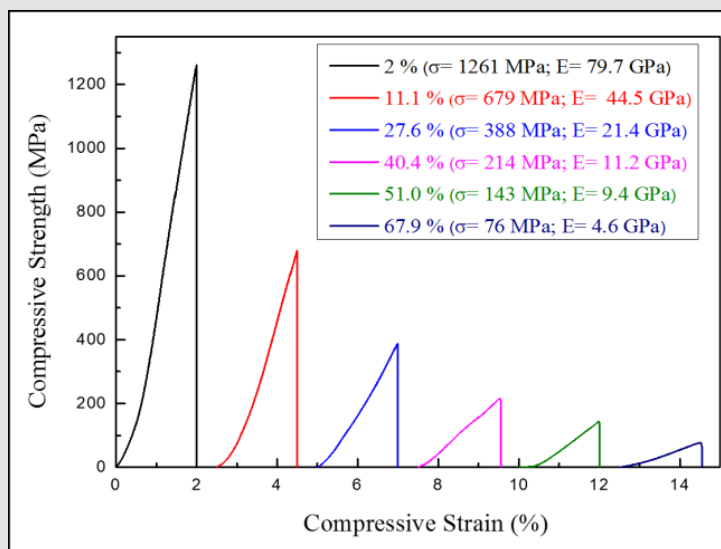


Figure 4: Compression stress-strain curves of TiZr-based BMG foams in various real porosities.

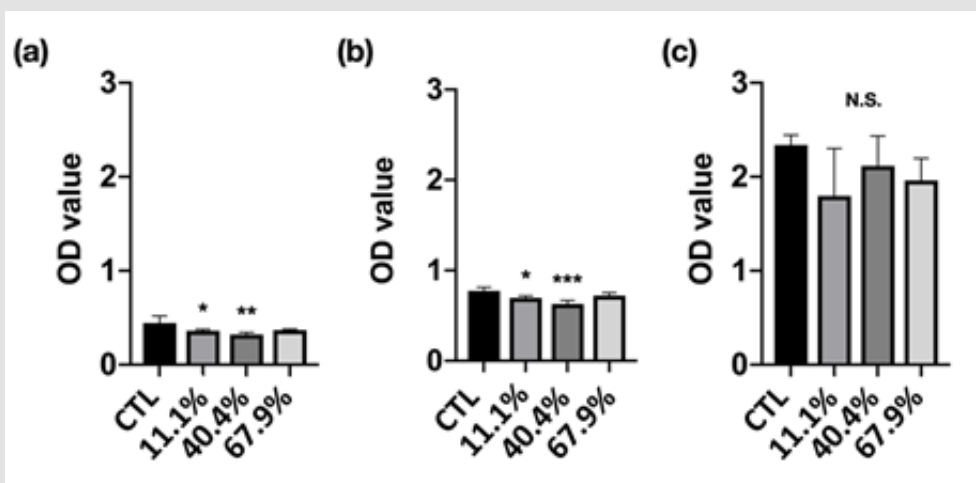


Figure 5: Cell viability of MC3T3-E1 pre-osteoblasts culture in standard medium and different precipitate media from immersion for

- (a) 1,
- (b) 3, and
- (c) 7 days incubation.

Table 1: Mechanical properties of TiZr-based BMG foams.

Real porosity (vol. %)	Young's modulus (E, GPa)	Compressive strength (σ, MPa)
0.0	112	1342
2.0	79.7	1261
11.1	44.5	679
27.6	21.4	388
40.4	11.2	214
51.0	9.4	143
67.9	4.6	76

### Biocompatibility Test

**Cell Viability:** Cell viability is used to determine the overall health of cells with a measure of the proportion of live and healthy cells in a population. The cell viability of MC3T3-E1 pre-osteoblasts cultured in the different precipitate medium was shown in Figure 5. The 11.1% and 40.4% groups demonstrated significantly lower cell viability at 1 and 3 days incubation. However, the cell viability at 7 days incubation has shown no difference compared with the control group (CTL). Fortunately, the OD value of each group has increased with incubation time increased, which means the cells were growing continuously, moreover, all groups can be classified as the first-level cytotoxicity according to ISO 10993-5 [18] (Figure 6).

**Migration Capacity:** Cell migration is an essential process involved in the major developmental stages of all complex organisms and results in the arrangement of cells into proper architecture, regulation of the nervous system, and formation of specialized organs and tissues. Figure 6 shows the migration capacity of MC3T3-E1 pre-osteoblasts culture with standard and different precipitate medium after scratch and 8 h after incubation. The gap distance was measured by Image J software to realize the migration of MC3T3-E1 pre-osteoblasts (Figure 6a). After 8 h of incubation, the gap distance has been reduced to around 600  $\mu\text{m}$ . However, there was no significant difference be found between each group (Figure 6b).

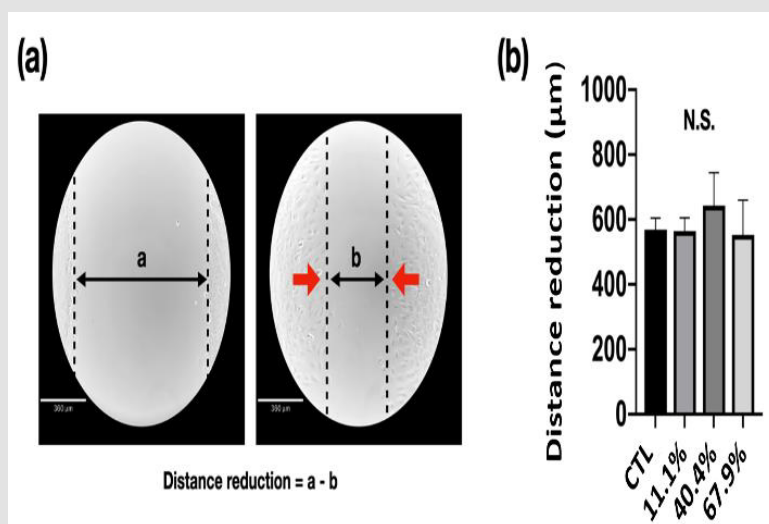


**Figure 6:** Migration capacity of MC3T3-E1 pre-osteoblasts cultured with alpha-minimum essential medium: (a) Cell migration at first scratch and after 8 h of incubation (CTL), and (b) The distance of gap has been reduced due to migration after 8 h of incubation.

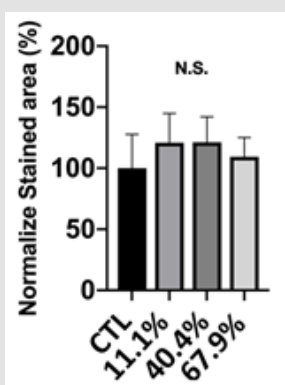


**Figure 7:** Extracellular matrix calcium and mineral deposition from MC3T3-E1 pre-osteoblasts treated with 11.1%, 40.4%, and 67.9% precipitate medium and stained by alizarin red S staining.

**Calcium Deposition:** For potential application as a bone implant in orthopedic fields, calcium deposition is the first cell functional response for testing. The quantitative analysis of the staining area by ARS dye after normalization is shown in Figure 7. The normalized calcium deposition rate of 11.1%, 40.4%, and 67.9% precipitate medium simulation was  $120 \pm 24\%$ ,  $121 \pm 20\%$ , and  $109 \pm 15\%$ , respectively (Figure 7). Yet, the statistical result shows that there was no significant difference between each group. The aforementioned results show that the calcium deposition rate of all groups always higher than 100% and this proves that the samples can positively be applied as bio-implant materials.

### Conclusion

In this study, the porous samples of TiZr-based BMG foams with porosities ranging from 11.1% to 67.9% were successfully

fabricated by Cu spacer particles. The pore size and morphology of TiZr-based BMG foams were similar with selected Cu spacer particles (100-120  $\mu\text{m}$ ) were confirmed after performing SEM examination. The TiZr-based BMG foams retain their amorphous structure after the hot pressing process based on XRD and TEM analysis. The mechanical properties of fabricated porous samples decreased with increasing the porosity of the samples. The cell viability increased with increasing incubation time and confirmed that the cell was growing continuously. The observed cell migration shows that the distance reduction is approximately 600  $\mu\text{m}$  after 8 h of incubation. In the calcium deposition rate, the values are always higher than 100% show that the samples are biocompatible to be applied to the human body.

## Acknowledgement

The authors gratefully acknowledge the analysis support from the Precision Instrument Center of National Central University and the biocompatibility equipment support from Taipei Medical University.

## References

1. B Basu, D Katti, Ashok Kumar (2009) Advanced Biomaterials: Fundamentals, Processing, and Applications. United States: A John Wiley & Sons, Inc pp. 768.
2. Q Chen, G A Thouas (2015) Metallic implant biomaterials. Materials Science and Engineering R: Reports 87: 1-57.
3. M Abdel-Hady Gepreel, M Niinomi (2013) Biocompatibility of Ti-alloys for long-term implantation. J Mech Behav Biomed Mater 20: 407-415.
4. M Geetha, A K Singh, R Asokamani, A K Gogia (2009) Ti based biomaterials, the ultimate choice for orthopaedic implants - A review. Progress in Materials Science 54(3): 397-425.
5. R Huiskes, H Weinans, B Van Rietbergen (1992) The relationship between stress shielding and bone resorption around total hip stems and the effects of flexible materials. Clin Orthop Relat Resn 274: 124-134.
6. S Nag, R Banerjee, HL Fraser (2005) Microstructural evolution and strengthening mechanisms in Ti-Nb-Zr-Ta, Ti-Mo-Zr-Fe and Ti-15Mo biocompatible alloys. Materials Science and Engineering C 25(3): 357-362.
7. A Inoue (2000) Stabilization of Metallic Supercooled Liquid. Acta Mater 48: 279-306.
8. AL Greer (2009) Metallic glasses...on the threshold. MaterialsToday 12(1-2): 14-22.
9. T Zhang, A Inoue (2002) Ti-based amorphous alloys with a large supercooled liquid region. Mater Sci Eng A 304-306(1-2): 771-774.
10. T Zhang, A Inoue (1998) Thermal and mechanical properties of Ti-Ni-Cu-Sn amorphous alloys with a wide supercooled liquid region before crystallization. Materials Transactions. JIM 39(10): 1001-1006.
11. DV Louzguine, A Inoue (2000) Nanocrystallization of Ti-Ni-Cu-Sn amorphous alloy. Scr Mater 43(4): 371-376.
12. A Peker, W L Johnson (1993) A highly processable metallic glass: Zr<sub>41.2</sub>Ti<sub>13.8</sub>Cu<sub>12.5</sub>Ni<sub>10.0</sub>Be<sub>22.5</sub> Appl Phys Lett 63: 2342-2344.
13. A Inoue, C Fan, T Masumoto (1995) Thermal Properties of Zr-TM-B and Zr-TM-Ga (TM=Co, Ni, Cu) Amorphous Alloys with Wide Range of Supercooling. Mater Trans JIM 36(12): 1411-1419.
14. JJ Oak, DV Louzguine-Luzgin, A Inoue (2007) Fabrication of Ni-free Ti-based bulk-metallic glassy alloy having potential for application as biomaterial, and investigation of its mechanical properties, corrosion, and crystallization behavior. J Mater Res 22(5): 1346-1353.
15. VT Nguyen (2019) Synthesis of biocompatible TiZr-based bulk metallic glass foams for bio-implant application. Mater Lett Vol 256.
16. VT Nguyen (2020) Open-cell tizr-based bulk metallic glass scaffolds with excellent biocompatibility and suitable mechanical properties for biomedical application. J Funct Biomater 11(2): 28.
17. CM Murphy, MG Haugh, FJ O'Brien (2010) The effect of mean pore size on cell attachment, proliferation and migration in collagen-glycosaminoglycan scaffolds for bone tissue engineering. Biomaterials 31(3): 461-466.
18. (1999) Standardization, I. O. f., ISO-10993-5: biological evaluation of medical devices part 5: Test for *in vitro* cytotoxicity methods. Arlington, VA: ANSI/AAMI.

ISSN: 2574-1241

DOI: 10.26717/BJSTR.2022.42.006821

Muhammad Jauharul Maqun. Biomed J Sci & Tech Res



This work is licensed under Creative Commons Attribution 4.0 License

Submission Link: <https://biomedres.us/submit-manuscript.php>



### Assets of Publishing with us

- Global archiving of articles
- Immediate, unrestricted online access
- Rigorous Peer Review Process
- Authors Retain Copyrights
- Unique DOI for all articles

<https://biomedres.us/>